Extension of the DF2016 isotropic model into an anisotropic ductile fracture criterion

IOP Conf. Series: Journal of Physics: Conf. Series **1063** (2018) 012148 doi:10.1088/1742-6596/1063/1/012148

Extension of the DF2016 isotropic model into an anisotropic ductile fracture criterion

Yanshan Lou[1] and Jeong Whan Yoon[1,2,*]

[1]Institute for Frontier Materials, Deakin University, 75 Pigdons Road, Waurn Ponds, VIC 3216, Australia
[2]Department of Mechanical Engineering, KAIST, 291 Daehak-ro, Yuseong-gu, Daejeon 305-701, Republic of Korea

j.yoon@deakin.edu.au / j.yoon@kaist.ac.kr

Abstract. The paper extends the recently proposed ductile fracture criterion of DF2016 (Lou, Chen, Clausmeyer, Tekkaya and Yoon, 2017. Modeling of ductile fracture from shear to balanced biaxial tension for sheet metals. International Journal of Solids and Structures 112, 169-184) to consider the anisotropic ductile fracture behaviour of sheet metals. The DF2016 criterion is coupled with the Hill48 yield function to model the anisotropy in ductile fracture. For the verification purpose, experiments are conducted for AA6082-T6 sheet with a thickness of 1.0 mm in various loading conditions: in-plane shear, uniaxial tension, plane strain tension, and the balanced biaxial tension. Tests are carried out in the rolling direction, diagonal direction and transverse direction. Fracture strains are measured by digital image correlation along different loading directions. The anisotropic fracture of the sheet is modelled by the DF2016 criterion by incorporating an anisotropic yield function. The predicted anisotropic fracture loci are compared with experimental results in shear, uniaxial tension, plane strain tension and balanced biaxial tension. The comparison demonstrates that the anisotropic DF2016 criterion accurately models the anisotropic fracture behaviour of AA6082-T6 sheet in wide loading conditions from shear to balanced biaxial tension.

1. Introduction

Ductile fracture is increasingly viewed as the cause of failure during forming of advanced high strength steels, aluminum alloys, titanium alloys and magnesium alloys [1, 2]. Dozens of ductile fracture criteria [3-11] were proposed in the last decade to model ductile fracture properties of these advanced metals. Recently, anisotropic behavior of metals was investigated extensively and some anisotropic ductile fracture criteria were proposed such as those by Luo et al. [12], Lou and Yoon [13, 14] and Park et al. [15].

In this study, the isotropic DF2016 criterion [9] is extended into an anisotropic form to couple the anisotropic effect on ductile fracture which is called “anisotropic DF2016 criterion”. For the verification purpose, experiments are conducted for AA6082-T6 (t=1.0 mm) to investigate ductile fracture under various stress states of pure shear, uniaxial tension, plane strain tension and the balanced biaxial tension. Fracture strains of these tests are measured by digital image correlation (DIC). The parameters of the anisotropic DF2016 criterion are calibrated with the measured fracture strains. The calibrated anisotropic DF2016 criterion is then utilized to model the dependence of ductile fracture on loading directions under various loading conditions. The predicted anisotropic dependence of ductile fracture is

then compared with experimental results to evaluate the accuracy of the proposed anisotropic DF2016 criterion.

2. Anisotropic DF2016 criterion

A shear ductile fracture criterion was proposed [9] to accurately characterize ductile fracture behaviour of sheet metals under four critical stress states of pure shear, uniaxial tension, plane strain tension and balanced biaxial tension. The proposed shear ductile fracture criterion is referred as the DF2016 isotropic criterion which is given in a form of

$$\left(\frac{2\tau_{max}}{\bar{\sigma}_{VM}}\right)^{C_1}\left(\left\langle\frac{f(\eta,L,C)}{f(1/3,-1,C)}\right\rangle\right)^{C_2}\bar{\varepsilon}_f^p = C_3 \quad \langle x\rangle = \begin{cases} x & if\ x \geq 0 \\ 0 & if\ x < 0 \end{cases} \tag{1}$$

with

$$f(\eta,L,C) = \eta + C_4\frac{(3-L)}{3\sqrt{L^2+3}} + C \tag{2}$$

In the DF2016 criterion of equation (1), τ_{max} denotes the largest shear stress, $\bar{\varepsilon}_f^p$ depicts the equivalent plastic strain to fracture, $\bar{\sigma}_{VM}$ represents the von Mises equivalent stress, η is used to represent the stress triaxiality and L is the Lode parameter. The DF2016 criterion assumes that the number of nucleated voids is a function of plastic deformation, the growth of voids is controlled by the stress triaxiality, the shape changing of voids is governed by the Lode parameter, and linking-up of voids is along the direction of the maximum shear stress as observed in various loading conditions from compressive upsetting to shear and tension of advanced metals [18]. Effect of void nucleation, growth, shape changing and shear linking-up on damage accumulation is modelled by four parameters introduced in equation (1): C_1, C_2, C_3 and C_4. In addition, the fifth parameter C is employed to consider the changeability of the cutoff value for the stress triaxiality, below which damage is not induced by plastic deformation. With the formulation derived in [16,17], effect of the Lode parameter is coupled in the proposed ductile fracture criterion by replacing the effect of the maximum shear stress as below:

$$\left(\frac{2}{\sqrt{L^2+3}}\right)^{C_1}\left(\left\langle\frac{f(\eta,L,C)}{f(1/3,-1,C)}\right\rangle\right)^{C_2}\bar{\varepsilon}_f^p = C_3 \tag{3}$$

It should be noted that the DF2016 criterion reduces to the DF2014 model when $C_4 = 1$, and the DF2012 criterion is recovered if $C_4 = 0$ and $C = 1/3$.

To extend the DF2016 criterion into an anisotropic form, the DF2016 criterion is modified into a form of

$$\left(\frac{2\tau_{max}}{\bar{\sigma}_{Hill48}}\right)^{C_1}\left(\left\langle\frac{f(\eta,L,C)}{f(2/3,1,C)}\right\rangle\right)^{C_2}\bar{\varepsilon}_f^p = C_3 \tag{4}$$

where $\bar{\sigma}_{Hill48}$ is the Hill48 plastic potential defined as

$$\bar{\sigma}_{Hill48} = \sqrt{F(\sigma_{yy}-\sigma_{zz})^2 + G(\sigma_{zz}-\sigma_{xx})^2 + H(\sigma_{xx}-\sigma_{yy})^2 + L\sigma_{yz}^2 + M\sigma_{zx}^2 + N\sigma_{xy}^2} \tag{3}$$

Six parameters are introduced in the Hill48 plastic potential. More anisotropic parameters can be introduced by substituting the Hill48 plastic potential by an advanced one, such as the Yld2004-18p function. The anisotropic parameters and the other coefficients introduced in the original DF2016 criterion are calibrated by fracture strains along different loading directions under various loading conditions of shear, uniaxial tension and plane strain tension measured from experiments.

3. Experiments for AA6082-T6

Experiments are conducted for AA6082-T6 to characterize the plastic and fracture behaviors of the alloy. Dogbone specimens are stretched along rolling direction (RD), diagonal direction (DD) and transverse direction (TD). The experimental *r*-values and anisotropy in strength under uniaxial tension are measured from the tensile tests of dogbone specimens. These experimental results are utilized to

calibrate the anisotropic Drucker yield function proposed by Lou and Yoon [11]. The anisotropic Drucker yield surfaces with the calibrated anisotropic parameters are compared with experimental results in Figures 1 and 2. It is obvious that the anisotropic Drucker yield function ($n = 2$) under associate flow rule accurately models the anisotropic behavior of the aluminum alloy with good agreement.

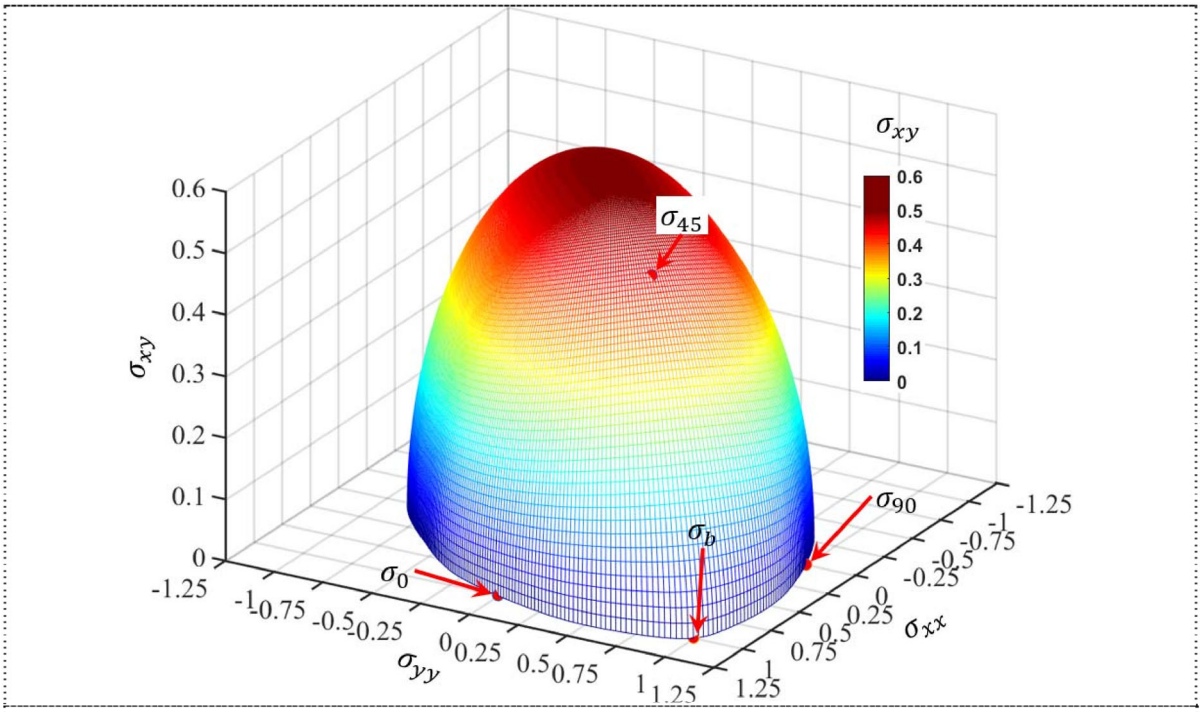

Figure 1. Comparison of the anisotropic Drucker yield surface ($n = 2$) under associate flow rule with experimental results of AA6082-T6.

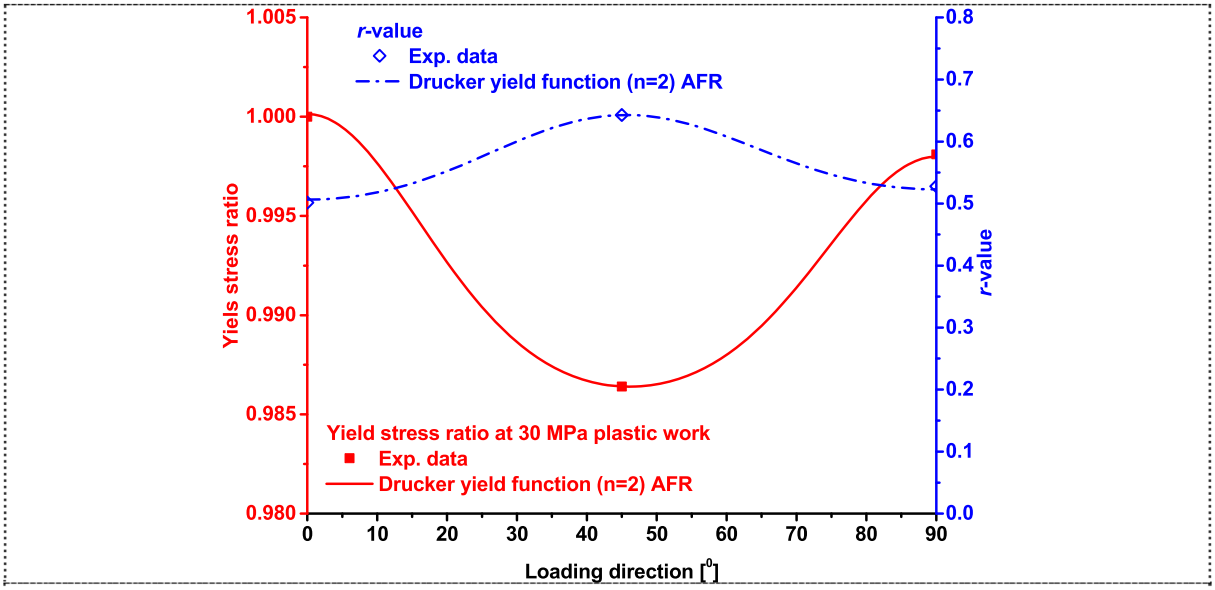

Figure 2. Comparison of uniaxial tensile yield stresses and r-values predicted by the anisotropic Drucker yield function ($n = 2$) under associate flow rule with experimental results of AA6082-T6.

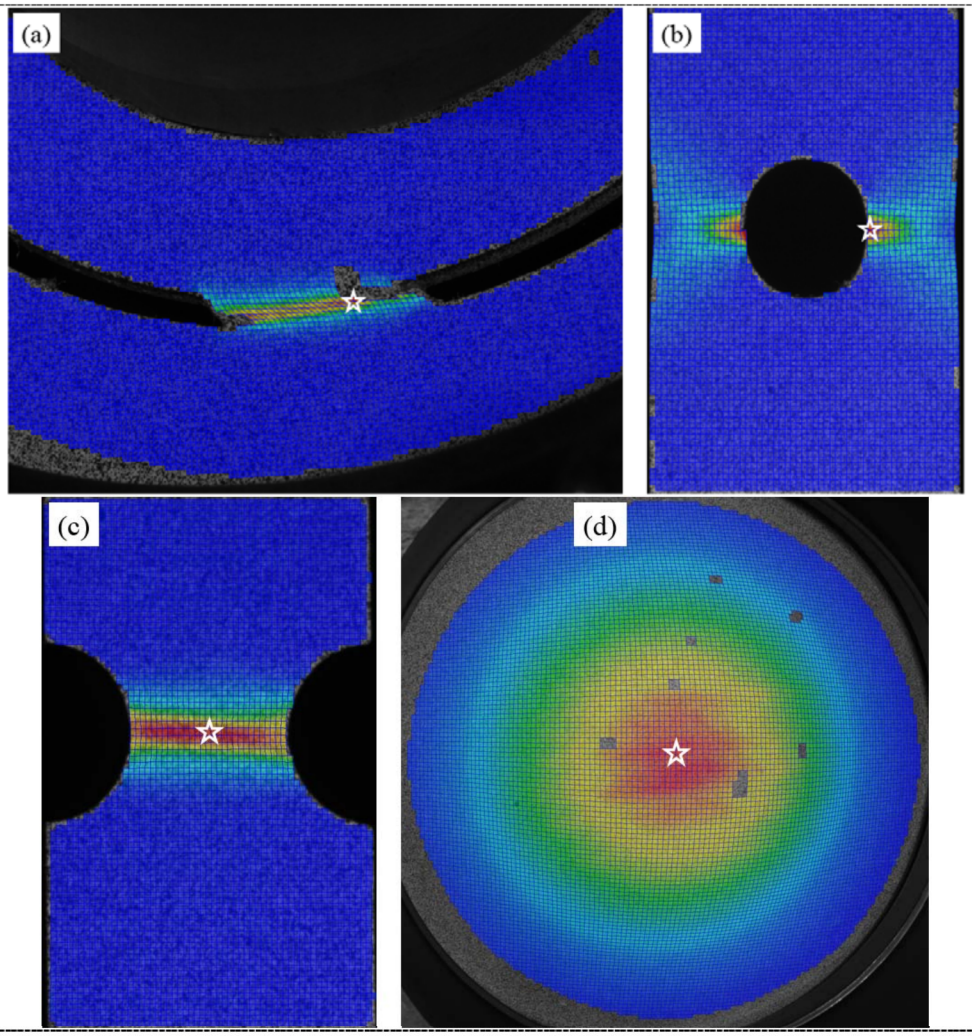

Figure 3. Specimens for the experimental measurement of fracture strains under various stress states: (a) in-plane torsion; (b) specimens with a central hole; (c) notched specimens; and (d) Nakajima tests.

Table 1. Fracture strains of the four types of tests in Figure 3.

In-plane torsion			Specimen with a central hole			Notched specimen			Nakajima
RD	DD	TD	RD	DD	TD	RD	DD	TD	test
0.6573	0.5663	0.6389	0.4166	0.4254	0.3576	0.3251	0.3209	0.2931	0.4988

The fracture behavior is investigated by four types of specimens in Figure 3: in-plane torsion test for pure shear, specimens with a central hole for uniaxial tension, notched specimens for plane strain tension, and the Nakajima test for the balanced biaxial tension. The in-plane torsion tests, specimens with a central hole and notched specimens are loaded along three different loading directions of RD, DD and TD to investigate effect of loading direction on ductile fracture. Stretching processes are recorded by 3D GOM Aramis system for the experimental measurement of fracture strains. The location for the measurement of fracture strains are depicted in Figure 3 by white stars. The von Mises equivalent plastic strains are measured right before the onset of ductile fracture for these tests and viewed as the fracture strains. The measured fracture strains are summarized in Table 1 for the calibration and verification of the anisotropic DF2016 criterion proposed in Section 2.

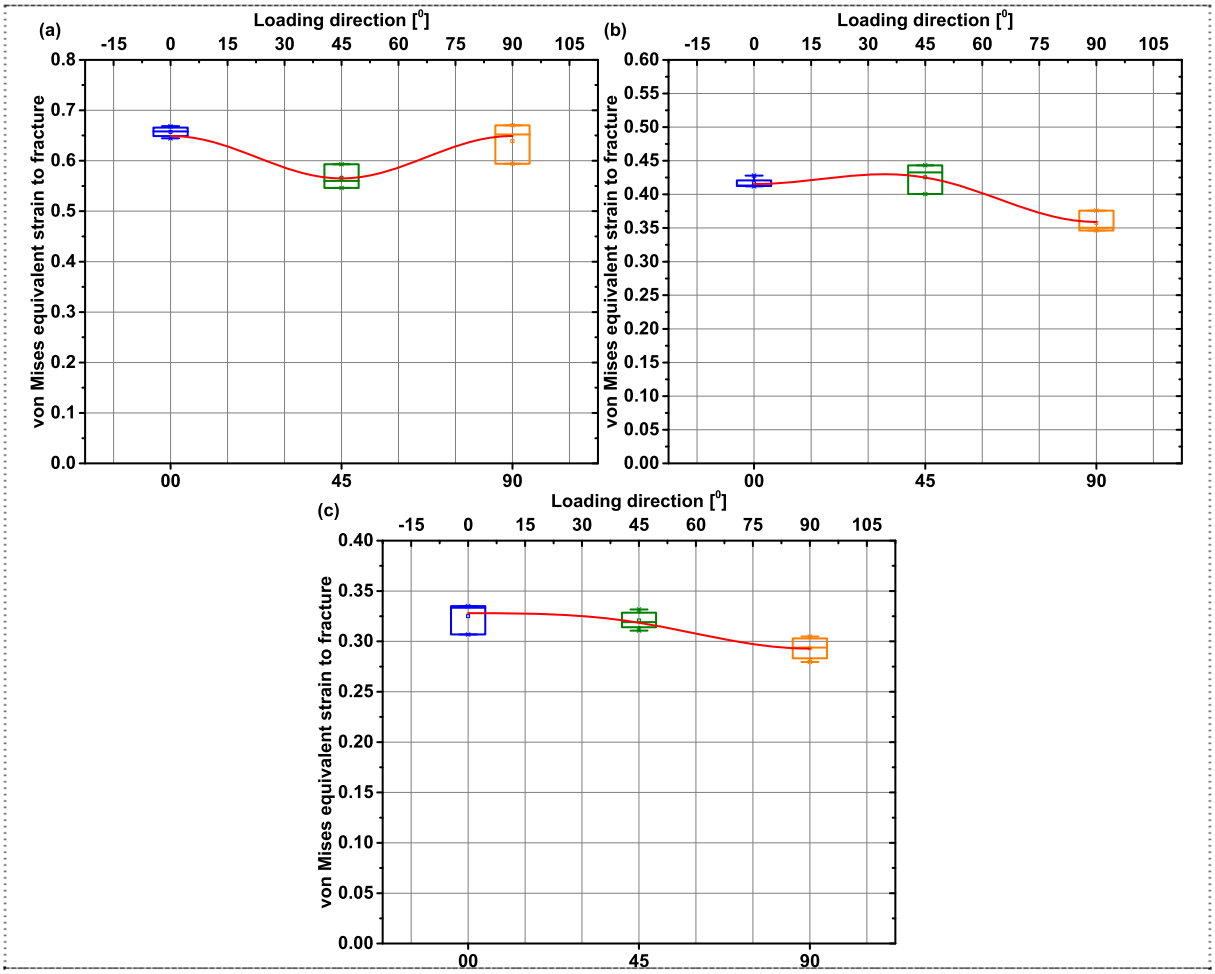

Figure 4. Comparison of the analytical fracture loci constructed by the proposed anisotropic DF2016 criterion with experimental results under various stress states: (a) in-plane torsion; (b) uniaxial tension; and (c) plane strain tension.

4. Application of the proposed anisotropic ductile fracture criterion to AA6082-T6

The fracture strains measured in Table 1 are then used to calibrate fracture coefficients of the proposed anisotropic DF2016 criterion introduced in Section 3. For the purpose of calibrations, the stress states of each tests are assumed to be ideal. That is, both the stress triaxiality η and the Lode parameter L are assumed to be 0 for in-plane torsion. For uniaxial tension, it is assumed that $\eta = 1/3$ and $L = -1$. For plane strain tension, these two parameters are set as $\eta = 1/\sqrt{3}$ and $L = 0$. For the Nakajima test, $\eta = 2/3$ and $L = 1$. Besides, the parameter C, which controls the cutoff value of the stress triaxiality, is assumed as $1/3$. Then the fracture coefficients are optimized as $C_1 = 1.4044$, $C_2 = 1.8040$, $C_3 = 0.4986$, $C_4 = 0.9910$, $F = 0.4779$, $G = 0.5721$, $H = 0.1947$, and $N = 1.0833$.

The fracture loci are constructed with the optimized fracture coefficients and compared with the experimental results in Figure 4 for various stress states of: (a) pure shear; (b) uniaxial tension; and (c) plane strain tension. The predicted fracture forming limit curve is compared in Figure 5 under biaxial tension along RD and TD. The experimental data points are explained in details in [19]. The comparison apparently proves that the proposed anisotropic DF2016 criterion predicts the anisotropic fracture behavior of the alloy with good agreement compared with experimental measurement under various loading conditions of pure shear, uniaxial tension, plane strain tension and the balanced biaxial tension for the aluminum alloy of AA6082-T6.

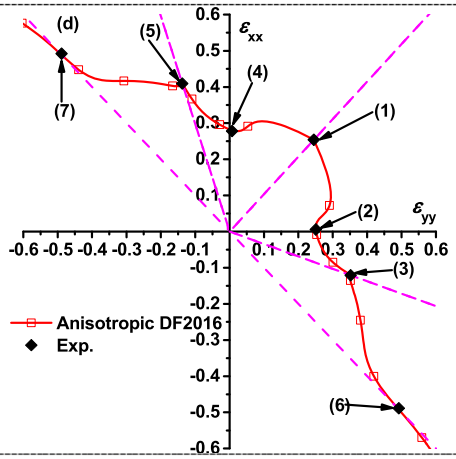

Figure 5. Comparison of the analytical fracture loci constructed by the proposed anisotropic DF2016 criterion with experimental results under biaxial tension along RD and TD.

5. Conclusions

In this paper, an anisotropic ductile fracture criterion is proposed based on the isotropic DF2016 criterion. The proposed anisotropic DF2016 criterion is verified by the experimental fracture tests of AA6082-T6 under various stress states of pure shear, uniaxial tension and plane strain tension as well as the balanced biaxial tension. Comparison of the constructed fracture loci by the anisotropic DF2016 criterion with experimental results reveals that the anisotropic DF2016 criterion provides satisfactory modelling of the anisotropic fracture behaviour of AA6082-T6. Considering its high accuracy, the anisotropic DF2016 criterion proposed is suggested to model the direction dependence of fracture behaviour of strong anisotropic metals during design and optimization of metal forming processes.

References

[1] Bao Y and Wierzbicki T 2004 *Int. J. Mech. Sci.* **46** 81.
[2] Lou Y and Huh H 2013 *J. Mater. Process. Technol.* **213** 1284.
[3] Bai Y and Wierzbicki T 2008 *Int. J. Plasticity* **24** 1071.
[4] Lou Y, Huh H, Lim S and Pack K 2012 *Int. J. Solids Struct.* **49** 3605.
[5] Isik K, Silva M B, Tekkaya A E and Martins P A F 2014 *J. Mater. Process. Technol.* **214** 1557.
[6] Lou Y, Yoon J W and Huh H 2014 *Int. J. Plasticity* **54** 56.
[7] Mohr D and Marcadet S J 2015 *Int. J. Solids Struct.* **67** 40.
[8] Hu Q, Li X, Han X and Chen J 2017 *Eur. J. Mech. A-Solid.* **66** 370.
[9] Lou Y, Chen L, Clausmeyer T, Tekkaya A E and Yoon J W 2017 *Int. J. Solids Struct.* **112** 169.
[10] Mu L, Zang Y, Wang Y, Li X L and Stemler P M A 2018 *Int. J. Mech. Sci.* **141** 408.
[11] Lou Y and Yoon J W 2018 *Int. J. Plasticity* **101** 125.
[12] Luo M, Dunand M and Mohr D 2012 *Int. J. Plasticity* **32** 36.
[13] Lou Y and Yoon J W 2017 *Int. J. Plasticity* **93** 3.
[14] Lou Y and Yoon J W 2015 *Key Eng. Mater.* **651-653** 163.
[15] Park N, Huh H, Lim S J, Lou Y, Kang Y S and Seo M H 2017 *Int. J. Plasticity* **96** 1.
[16] Lou Y and Huh H 2013 *Acta Mech. Solida Sin.* **26** 642.
[17] Lou Y and Huh H 2013 *Int. J. Solids Struct.* **50** 447.
[18] Lou Y, Yoon J W, Huh H, Chao Q and Song J H 2018 *Int. J. Mech. Sci.* doi.org/10.1016/j.ijmecsci.2018.03.025.
[19] Lou Y and Yoon J W 2018 *Int. J. Solids Struct.* under review.